

BVI-VFI: A Video Quality Database for Video Frame Interpolation

Duolikun Danier, *Student Member, IEEE*, Fan Zhang, *Member, IEEE*, and David R. Bull, *Fellow, IEEE*

Abstract—Video frame interpolation (VFI) is a fundamental research topic in video processing, which is currently attracting increased attention across the research community. While the development of more advanced VFI algorithms has been extensively researched, there remains little understanding of how humans perceive the quality of interpolated content and how well existing objective quality assessment methods perform when measuring the perceived quality. In order to narrow this research gap, we have developed a new video quality database named BVI-VFI, which contains 540 distorted sequences generated by applying five commonly used VFI algorithms to 36 diverse source videos with various spatial resolutions and frame rates. We collected more than 10,800 quality ratings for these videos through a large scale subjective study involving 189 human subjects. Based on the collected subjective scores, we further analysed the influence of VFI algorithms and frame rates on the perceptual quality of interpolated videos. Moreover, we benchmarked the performance of 28 classic and state-of-the-art objective image/video quality metrics on the new database, and demonstrated the urgent requirement for more accurate bespoke quality assessment methods for VFI. To facilitate further research in this area, we have made BVI-VFI publicly available at <https://github.com/danielism97/BVI-VFI-database>.

Index Terms—Video quality database, subjective quality assessment, video frame interpolation, perceptual quality, BVI-VFI.

I. INTRODUCTION

Video frame interpolation (VFI) is an important video processing technique which is used to synthesise intermediate frames between every two consecutive frames in a video sequence. VFI offers utility, and has been the subject of increased popularity, across many applications in recent years; these include slow motion generation [1], video compression [2], medical imaging [3] and animation production [4]. Driven by the development of various deep learning techniques and more powerful computational hardware, there has been a surge in the reporting of new video frame interpolation methods, which are generally classified into two groups: flow-based and kernel-based. While flow-based methods rely on optical flow to warp reference frames, kernel-based approaches estimate local interpolation kernels to synthesise output pixels. Although these VFI approaches have delivered significant improvements in terms of interpolation performance [5–10],

challenging scenarios still exist that cause interpolation failure; these often relate to content containing large motions, dynamic textures, and occlusions [6].

While there is ongoing activity to develop new VFI methods that tackle these challenges, the perceptual quality assessment of frame interpolated content remains underinvestigated. Currently, the most widely adopted approach for assessing VFI performance is to calculate the distortion between the interpolated frames and their original ground-truth counterparts using image quality assessment (IQA) models including PSNR, SSIM [11], and LPIPS [12]. More recently, new perceptually oriented image and video quality metrics have been developed for other applications such as video compression, with notable examples including VSI [13], DISTS [14], VMAF [15], FAST [16] and C3DVQA [17]. However, none of these models has been fully evaluated on frame interpolated videos against subjective ground truth. Due to this concern, in order to accurately assess VFI performance, some researchers [6, 18] have resorted to benchmarking based on subjective opinion scores through psychophysical experiments; these however are very time consuming and resource-heavy. In this context, there is an urgent need to develop a video quality database containing diverse frame interpolated content alongside reliable subjective score metadata, which can be employed to investigate the competence of existing image and video quality metrics for the VFI task.

Although there have been little reports of research in this area [19, 20], the associated databases either contain human opinion scores only on single interpolated images, or only focus on slow-motion videos at a fixed frame rate. Also, the video sequences in [20] suffer from compression artefacts in addition to VFI-related distortions, making it difficult to decouple these during assessment. We have previously addressed these issues in [21], where a small video quality database for VFI was developed based on a limited subjective study and a benchmark experiment only involving a few objective quality metrics. To overcome these limits and make further progress in understanding the perceptual quality of frame interpolated videos, in this paper we extend our previous work [21] and present a new video quality database, BVI-VFI, which contains 540 interpolated videos generated by various VFI algorithms, covering different frame rates, spatial resolutions and diverse content types. The database also includes subjective quality scores for all videos collected through a large-scale subjective experiment. Based on the subjective data, we performed a much more comprehensive evaluation of existing objective quality metrics, involving 28 conventional and learning-based image and video quality models. The primary contributions

This work involved collecting data from human participants. The relevant experiments have been approved by the Faculty of Engineering Research Ethics Committee of the University of Bristol (Ref 10739; PI: David R. Bull; Title: Subjective Quality Study on Video Frame Interpolation).

The authors are with the Bristol Vision Institute, University of Bristol, Bristol BS8 1TH, U.K. (e-mail: duolikun.danier@bristol.ac.uk; fan.zhang@bristol.ac.uk; dave.bull@bristol.ac.uk).

The authors acknowledge the funding from China Scholarship Council, the University of Bristol and the UKRI MyWorld Strength in Places Programme.

are summarised below.

- We developed the first bespoke video quality database for frame interpolation, BVI-VFI, that covers multiple frame rates (30-120fps) and spatial resolutions (540p-2160p). It contains 540 distorted sequences generated by five different video frame interpolation methods from 36 source videos, which uniformly cover a wide range of video features.
- We conducted a large-scale laboratory-based psychophysical experiment to collect subjective quality ground truths for all the videos in BVI-VFI.
- We performed quantitative comparison of 28 classic and state-of-the-art image/video quality assessment methods on the BVI-VFI database. Cross-validation experiments were also performed for learning-based metrics.
- The proposed new database serves as an important platform for developing and validating new quality metrics for video frame interpolation. It can also be used as a test dataset for benchmarking VFI algorithms due to its content diversity.

The rest of the paper is organised as follows. We first briefly review the relevant literature in Section II, and then describe the process of source video collection and test sequence generation in Section III. The subjective experiment, the data processing procedures and analysis of the collected subjective opinions are presented in Section IV. Section V summarises the comparative study results for 28 quality assessment methods. Finally, Section VI draws conclusions and outlines potential future work.

II. RELATED WORK

In this section, we first describe previous works in video frame interpolation, and then summarise the related research work on objective video quality metrics and subjective quality assessment in the context of VFI.

A. Video Frame Interpolation

Early attempts [22, 23] to perform video frame interpolation typically used estimated optical flow maps to warp input frames. This paradigm, referred to as flow-based VFI, was further developed in the learning-based VFI literature [24]. These methods adopted various techniques to enhance interpolation quality, including the use of contextual information [25], designing bespoke flow estimation module [1, 7, 8, 24, 26–29], employing a coarse-to-fine refinement strategy [30–33], developing new warping operations [9, 34, 35] and adopting higher-order motion modelling with additional input frames [5, 10, 36]. Some researchers argue that the imposition of a one-to-one mapping between the target and source pixels can limit the ability of flow-based methods to handle complex motions. This has led to the development of kernel-based methods [37–46] that predict adaptive local interpolation kernels to synthesise the output pixels. This creates a many-to-one mapping between the source and target pixels, supporting additional degrees of freedom. Moreover, other researchers reported the limitations of predicting fixed-shaped kernels [37, 38], and introduced

deformable kernels [47] to achieve improved interpolation performance. Finally, observing that fixed kernel sizes can limit the captured motion magnitude, some VFI methods [6, 48, 49] combine flow-based and kernel-based approaches in a single framework to benefit from both model types.

Besides the flow-/kernel-based classes, other VFI paradigms exist, for example based on pixel hallucination [18, 50], phase information [51, 52], event cameras [53–55], unsupervised learning [56, 57], and meta-learning [58]. More recently, the joint problem of deblurring and interpolation has also been addressed in [59, 60].

B. Objective Quality Assessment for VFI

In the current VFI literature, the commonly adopted approach for benchmarking interpolation performance is to measure the distortion between an interpolated video and its ground-truth version. The most popular measurement methods are PSNR, SSIM [11] and LPIPS [12], all of which are applied at the level of a single image or frame. There are also many image/video quality metrics developed for other application scenarios, including approaches based on classic signal processing methods, such as MS-SSIM [61], VIF [62], VSI [13], FAST [16], SpEED [63], ST-RRED [64]. More recently, machine learning techniques have been employed in the development of perceptual metrics including VMAF [15], C3DVQA [17] and CONTRIQUE [65]. Alongside these generic quality metrics, assessment methods that were designed to specifically model the effect of frame rate/spatial resolution down-sampling or frame interpolation have been reported, including FRQM [66], ST-GREED [67], VSTR [68], FAVER [69] and FloLPIPS. However, none of these methods have been rigorously benchmarked due to the lack of databases with diverse content and ground-truth metadata.

C. Subjective Quality Assessment for VFI

Various subjective quality databases exist that support studies into how the human vision system (HVS) perceives video quality. These include those developed in the context of video compression, e.g., the early VQEG FR-TV Phase I [70], LIVE VQA [71], LIVE Mobile [72], CSIQ-VQA [73], BVI-HD [74], LIVE-SJTU [75], TVG [76], CSCVQ [77] and LIVE Livestream [78]. Video quality databases also exist that support investigations into distortions due to video parameter variations (e.g, frame rate, spatial resolution and bit depth, with or without video compression artefacts), including MCL-V [79], MCML-4K-UHD [80], BVI-SR [81], BVI-HFR [81], BVI-BD [82], FRD-VQA [83], LIVE-YT-HFR [84], AVT-VQDB-UHD-1 [85] and ETRI-LIVE STSVQ [86].

There are, however, very few examples of databases that contain content distorted by different VFI methods; the most relevant contributions being [19] and [20]. In [19], subjective quality scores were collected by showing viewers individual interpolated frames instead of video sequences. This methodology is limited since it does not consider temporal artefacts which could significantly influence the perceived video quality [87]. The later database, KosMo-1k [20], addresses this issue by collecting subjective opinions when viewing

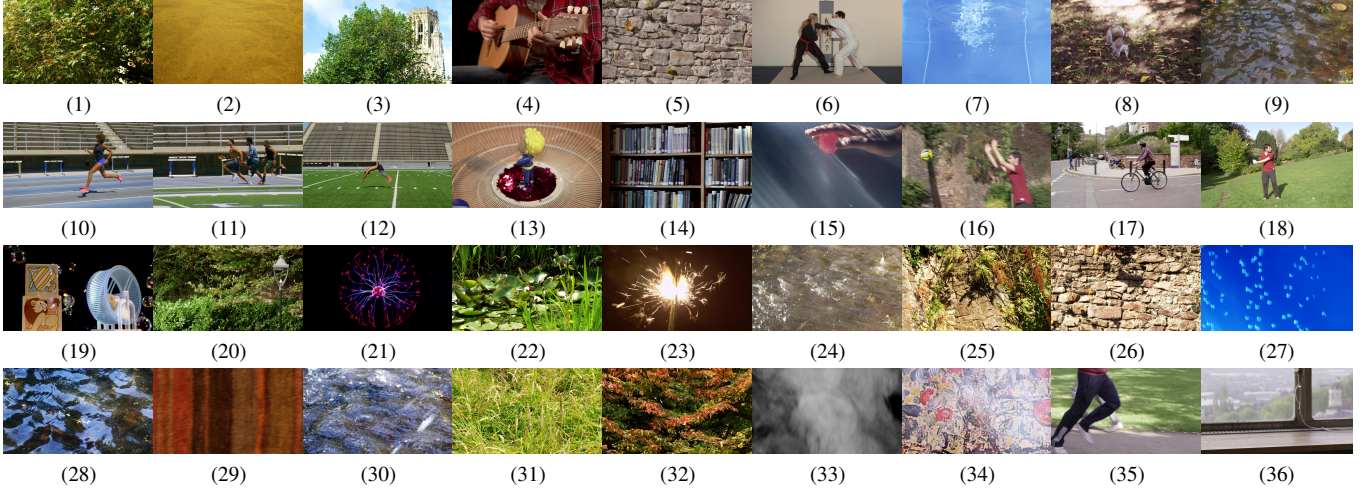


Fig. 1. Sample frames from the 36 source sequences of the BVI-VFI database. (1)-(12): sequences at 960×540 . (13)-(24): sequences at 1920×1080 . (25)-(36): sequences at 3840×2160 .

TABLE I
THE UNIFORMITY AND RANGE CHARACTERISTICS OF THE 36 SOURCE SEQUENCES IN THE BVI-VFI DATABASE.

Feature	SI	TI	CF	DTP	MV
Uniformity (0-1)	0.93	0.85	0.95	0.87	0.87
Range (0-1)	0.88	0.97	0.74	0.99	0.99

interpolated videos. However, the video sequences were played in slow-motion (one specific use case of VFI) and, in addition, all the distorted sequences were contaminated by video compression artefacts, making it difficult for subjects to isolate VFI artefacts. Due to their disadvantages, none of these databases can be recommended for evaluating the performance of VFI quality metrics. Hence there is an urgent requirement for a bespoke video quality database. We address this need in the following section.

III. THE BVI-VFI DATABASE

This section describes the approach used to select the source sequences in the BVI-VFI database, and how the test videos were generated.

A. Reference Sequences

The BVI-VFI database contains 108 reference sequences in total, which were generated from 36 different source videos captured at 120fps and resampling them to 60 and 30 fps. The 36 source videos have three different spatial resolutions: 12 at 3840×2160 (UHD-1), 12 at 1920×1080 (HD), and 12 at 960×540 . For each resolution group, we: (i) first created a selection pool consisting of 120fps, YUV 4:2:0 8 bit video candidates collected from various sources; (ii) then calculated five video features: Motion Vector (MV), Dynamic Texture Parameter (DTP), Spatial Information (SI), Temporal information (TI) and Colourfulness (CF) for each candidate; (iii) used the selection algorithm described in [74] to determine the final source sequences in the BVI-VFI database. Among all these

five features, MV and DTP describe the overall motion magnitude and complexity in the video which are highly relevant to VFI. The other three features are commonly employed to characterise the properties of video databases [81, 84, 86]. The calculation of MV, SI, TI and DTP can be found in [88, 89], and DTP is described in [74].

All 22 HD source candidates (in YUV 4:2:0 8 bit 120fps format) came from the BVI-HFR dataset [81]. They were first truncated to five seconds following the research study in [89]. Twelve¹ sequences were selected from this pool using the algorithm in [74] to ensure wide feature coverage range and uniform feature distribution [88] across the whole database². We then performed the same procedure for the UHD-1 resolution group, for which 27 source candidates were collected from a variety of sources, including five from the LIVE-YT-HFR dataset [84], six from the UVG dataset [90], and 16 videos captured using a RED Epic-X video camera at the University of Bristol. All these sequences were also trimmed to five seconds (600 frames) and converted to YUV 4:2:0 8 bit format to ensure consistency with the abovementioned HD sources. In addition, because of the limited spatial resolution (up to 1920×1080) of the high frame rate display employed in the subjective experiment, we further cropped HD representations of these UHD-1 videos. Specifically, we generated 9 cropped candidates for each UHD-1 video ($x \in \{0, 960, 1920\}$, $y \in \{0, 540, 1080\}$ where (x, y) is the top-left coordinate of the crop), and selected the crop that has the highest content similarity to the original UHD-1 video in terms of two feature descriptors: MV and DTP. By doing so, we obtain 27 cropped videos, which retain the characteristics of UHD-1 content despite their smaller spatial extent. From these 27 sources, we selected 12 UHD-1 source videos using the same procedure as for the HD resolution group. For the

¹The number of source sequences for each resolution group was determined based on the trade off between available resources for computation and subjective testing, and the optimisation of feature uniformity and range values.

²The preliminary results based on HD reference and distorted sequences have been published in [21].

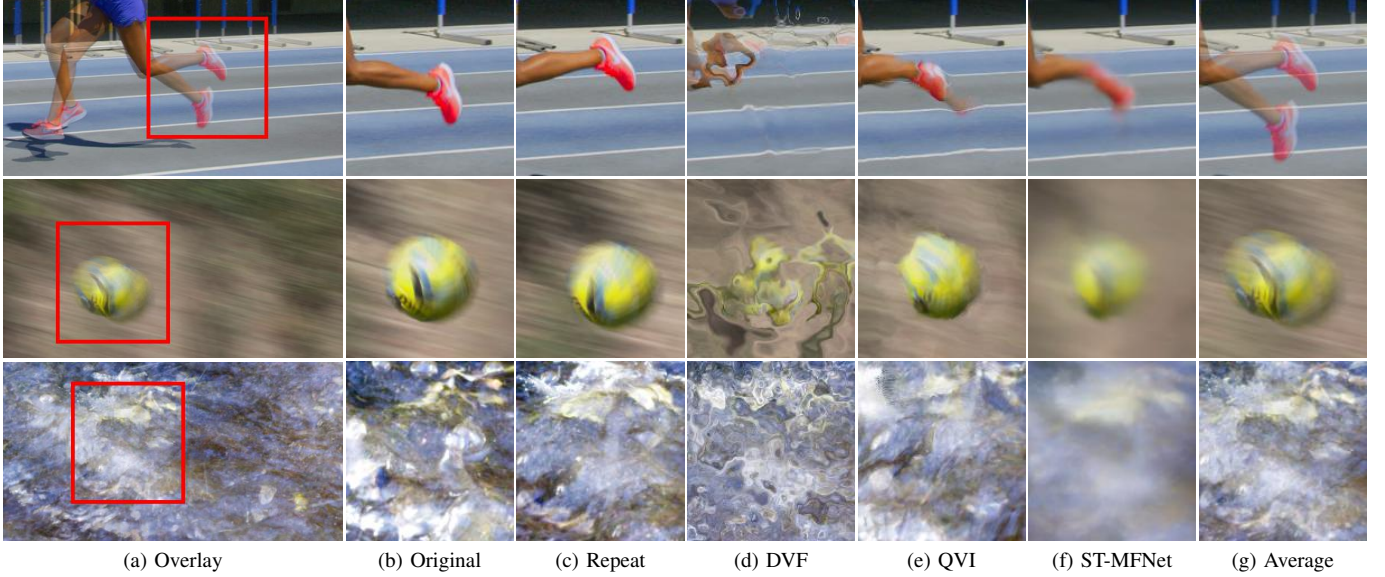


Fig. 2. Example frame blocks generated by five VFI algorithms. It is noted that for frame repeating, although the result appears less distorted, the video exhibits motion juddering.

resolution group of 960×540 , due to the lack of publicly available 120fps videos at this resolution, we generated a selection pool by spatially down-sampling (using a Lanczos3 filter) the unused 120fps videos from the previously collected HD and UHD-1 candidates. Then we applied again the same sequence selection process to obtain the 12 source sequences at 960×540 .

Finally, to obtain reference sequences sampled at various frame rates, the twelve 1920×1080 , twelve cropped 3840×2160 and the twelve 960×540 source videos at 120fps were temporally sub-sampled to 60fps and 30fps by frame dropping, resulting in 108 references. An alternative sub-sampling method, frame averaging, can create visible ghosting artefacts in cases with small shutter angles and introduce additional motion blur. Both of these artefacts can seriously deteriorate the frame interpolation performance [59, 60]. In contrast, although frame dropping reduces the original shutter angle which may introduce motion judder, the resulting frames provide a superior basis for VFI applications. Sample frames of the all the final source sequences are shown in Fig. 1. Table I reports the range and uniformity characteristics of the source sequences in BVI-VFI. It can be observed that the selected source sequences offer a wide and uniform coverage for all the spatial and temporal features measured.

B. Distorted Sequence Generation

To generate different distorted versions of the 108 reference sequences, we first halved their frame rates by dropping every second frame, and then reconstructed the dropped frames using five VFI algorithms: frame repeating, frame averaging (where the middle frame is generated by averaging every two frames), DVF [26], QVI [5] and ST-MFNet [6]. The first two methods were included because they have very low computational complexity and produce unique artefact types, motion judder and motion blur respectively. The other three

algorithms are all based on deep learning. DVF is one of the early methods that estimates the optical flow between the non-existent middle frame and its neighbouring frames using a simple linear approximation. QVI is a more advanced approach that employs a second-order motion model. Finally, ST-MFNet is a recent state-of-the-art approach that combines flow-based warping and kernel-based synthesis to allow more complex pixel transformation. For the deep learning-based models, we employ the model parameters pre-trained as in [6] due to their proven performance on various challenging content. As a result, a total of 540 (108×5) distorted videos were obtained. Fig. 2 shows example frames interpolated by all five VFI methods, where it can be seen that diverse artefacts types have been generated. It should be noted that we did not employ video compression during the test sequence generation process, hence our content is free from compression artefacts, ensuring a focus solely on the perceptual quality of VFI-generated content.

IV. SUBJECTIVE EXPERIMENTS

In order to collect quality scores for the sequences in BVI-VFI, we conducted a large-scale subjective test, which is described in this section.

A. Experimental Setup

The psychophysical experiment was conducted in a darkened laboratory-based environment set up according to [91]. The sequences were displayed on a BENQ XL2720Z high frame rate monitor with a screen size of 598×336 mm. The spatial and temporal resolutions of the display were set to 1920×1080 and 120fps. Note that all sequences were played back at their native spatial and temporal resolutions. The viewing distance was set to 1008mm, which is three times the picture height for HD and cropped UHD-1 sequences and

six times the picture height for 540p sequences. These are all compliant with ITU-R BT.500-14 [91]. The monitor was connected to a Windows PC, with Matlab Psychtoolbox 3.0 software [92] used to control the experiment and collect user input from a wireless mouse.

B. Experimental Procedure

We employed the Double Stimulus Continuous Quality Scale (DSCQS) methodology [91] for this subjective experiment. In each trial of a session, the subject is presented with two sequences, A and B, one of which is the reference sequence and the other is a distorted version generated by one of the VFI algorithms. The display order of the reference and distorted videos is randomised, and the subject is unaware of which one is the reference. Sequences A and B are shown to the subject twice in an alternating fashion (i.e., A, B, A, B) interleaved with grey screens containing text informing the subject which video (A or B) will be played next. After videos are played, the subject is presented with a grey screen showing the question: “Please rate the quality of video A” and another such question for video B. The user is then asked to provide their answers using two continuous sliders (for A and B) with five evenly spaced ticks labelled *Bad*, *Poor*, *Fair*, *Good*, *Excellent*, which correspond to 0, 25, 50, 75, 100 respectively. The slider is controlled via a mouse. There are two-second grey-screen intervals between video presentations, and the rating process of the viewers are not timed.

A total of 189 subjects were paid to participate in this experiment. In order to reduce viewer fatigue caused by excessively long experiment sessions while ensuring sufficient raw subjective scores (at least 20) for each distorted video, we divided the participants into nine groups and each group of subjects were presented with sequences associated with only four source content types, which include 60 (4 content \times 3 frame rates \times 5 VFI methods) distorted sequences and their reference counterparts.

In the test session, each participant was presented with 60 different trials (in randomised order), and each distorted video was rated by at least 20 subjects. At the beginning of each session, the participant was assessed for visual acuity with a Snellen chart and colour blindness with an Ishihara chart. The subject was then briefed about the experiment and given detailed instructions. To further familiarise him/her with the experiment, four practice trials were then performed, which contain different sequences from those in BVI-VFI. Finally, each formal test session took approximately 30 minutes on average.

C. Data Processing and Validation

As mentioned above, each of the 189 participants took part in only one session consisting of 60 trials. This resulted in 60 pairs of scores given by each subject for the 60 reference-distortion tuples, and each trial (reference-distortion pair) was rated by at least 20 subjects. We then processed these raw scores following the procedures specified in [91] to obtain Differential Mean Opinion Score (DMOS) values for each test sequence. Specifically, we first computed the differential

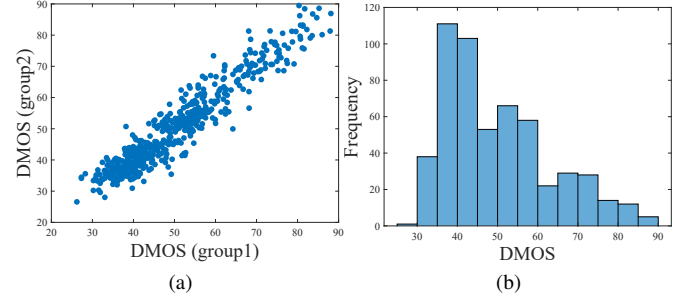


Fig. 3. (a) Scatter plot of DMOS values given by two randomly separated equal-size groups of subjects. (b) Histogram of all the DMOS values.

opinion scores for each distorted video by taking the difference between the scores given by each subject to that video and its reference counterpart. Then the Z-scores [93] are computed by normalising the scores given by each subject. The Z-scores obtained are used to perform subject screening, the procedure for which is described in details in [91]. This screen approach first tests for the normality of the scores received by the videos, then assesses for each subject whether her/his scores fall well enough within the distribution of all scores.

After repeating this process for all the 189 subjects, nine were found eligible for rejection. In order to further confirm the credibility of the final data, we additionally analysed the inter and intra-subject consistencies [94] after linearly re-scaling [84, 86] the Z-scores to the range [0, 100]. The DMOS value for each distorted video were obtained by

$$\text{DMOS}_j = \frac{1}{N_j} \sum_{i=1}^{N_j} z_{ij} \quad (1)$$

where j indexes the distorted video, N_j is the number of judgements given to video j , z_{ij} is the difference between the scores given by subject i to the reference version of video j and to video j .

The inter-subject consistency [94] is assessed by measuring the correlation between the average differential scores (DMOS) given by two randomly separated equal-size groups of subjects. Due to the subject grouping described, the random split was performed within each group. We performed 1000 times of such random split and at each time computed the Spearman’s Ranked Order Correlation Coefficient (SROCC) between the DMOS of the two groups. The median SROCC value for the 1000 splits was found to be 0.926, and the standard deviation was 0.004. This indicates a high level of consistency among subjects. Fig. 3 (a) shows the distribution of the average differential values for one such split.

Furthermore, we also checked the intra-subject consistency [94], which is a measurement of how well the judgement of each subject agrees with all the viewers who viewed the same videos. This is evaluated by calculating the SROCC between the differential scores given by each subject to his/her allocated videos and the DMOS values given by the group for the same videos. Performing this process for every subject, we obtained a median SROCC value of 0.778 with a standard deviation of 0.106, which are reasonable values that indicate high reliability of the collected opinion scores [84].

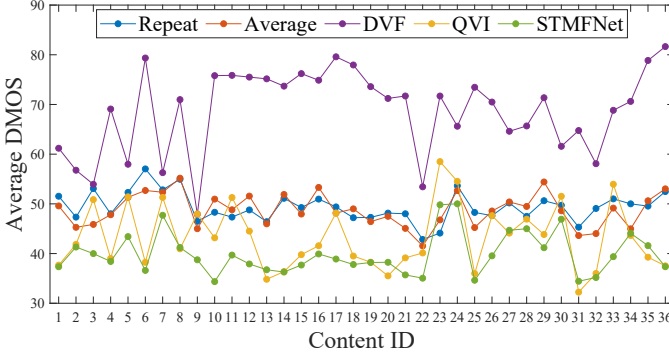


Fig. 4. The average DMOS values for each employed VFI algorithm on every source sequences (the Content ID here refers to Fig. 1.)

Finally, Fig. 3 (b) shows a histogram of all the DMOS values calculated using Equation (1). The mean and the standard deviation of the DMOS values were 50 and 13.32. The maximum and minimum DMOS values were 87.53 and 26.39.

D. Analysis of Subjective Data

To investigate the performance of the five VFI algorithms on different source content, we plot the average DMOS³ achieved by each method for all the source sequences in Fig 4. It is noted that lower DMOS values indicate better perceptual quality. We can observe that in general, the more recent deep learning (DL)-based VFI methods, ST-MFNet and QVI, achieved the lower DMOS values, with ST-MFNet performing the best in most cases. The other employed DL-based method, DVF, received the highest overall DMOS values, which may be due to the assumption of simple linear motion between adjacent frames in the DVF approach, i.e. the optical flows from the interpolated middle frame to both of its neighbouring frames are constrained to be symmetric. Such an assumption clearly fails in scenarios with non-linear motions, which exhibit in many sequences in the BVI-VFI database. The two non-DL methods, frame repeating and averaging, achieved similarly mediocre average DMOS values at around 50.

It can also be observed that there are several scenes where the simple non-DL methods achieve similar or even better perceived quality than the two best-performing DL-based algorithms. Most of these scenarios involve dynamic textures [95], which exhibit rapid and irregular motions of unstructured entities, such as leaves (sources 3, 5), water (sources 7, 9, 24, 28, 30), fire (source 23) and smoke (sources 33 and 34). There are two reasons for this. Firstly, such complex motions, sometimes combined with large motion magnitude, are too challenging for these two advanced DL-based algorithms QVI and ST-MFNet, causing them to produce frames with unacceptable quality and obvious interpolation artefacts. Secondly, the texture masking effect introduced by such dynamic textures decreases the sensitivity of human eyes, thus making it difficult to distinguish between different distortions and resulting in similar levels of perceived quality. The images on the third row of Fig. 2 (which correspond to source 30) illustrate both

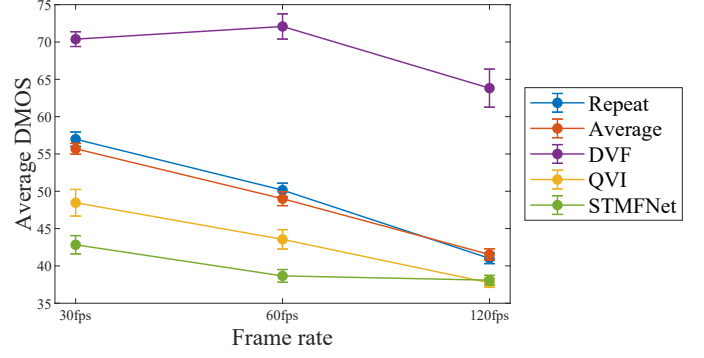


Fig. 5. The average DMOS values for each VFI algorithm at different frame rates. The error bars denote the standard error over sequences.

scenarios, where the complex scene of splashing water exhibits texture masking and poses significant challenges to DL-based VFI methods.

We also analysed the effect of frame rate on the interpolation quality. Fig. 5 plots the average DMOS values achieved by each algorithm among all source sequences against frame rate. It shows that the difference in the average DMOS values achieved by the state-of-the-art DL-based methods and those obtained by the simple non-DL methods becomes smaller at higher frame rates. It is reasonable to conjecture that, at even higher frame rates, this difference can become negligible and the computationally heavy DL-based methods can be replaced by simple frame repeating or averaging. However, this needs to be confirmed by further study.

V. EVALUATION OF OBJECTIVE QUALITY METRICS

One of the key motivations for developing the new BVI-VFI database is to provide a rigorous framework for evaluating the performance of quality assessment metrics on frame interpolated content. In this section, we perform a comprehensive evaluation with 28 conventional and state-of-the-art image and video quality assessment methods. While the majority of the tested metrics are full/reduced-reference models (which make use of certain information from the pristine reference frames), several no-reference ones (which predict the quality solely based on the distorted frames) are also included.

The full-reference quality metrics evaluated in this experiment include the most commonly used metrics in the VFI literature, namely PSNR, SSIM [11] and LPIPS [12]. While PSNR and SSIM are conventional methods, LPIPS is a deep learning-based method that measures distortion in deep feature space. Additionally, we evaluated other popular conventional image quality metrics including MS-SSIM [61], VIF [62], VSI [13], FSIM [96], GMSD [97], and deep learning-based ones: DISTS [14], PieAPP [98], DeepIQA [99] and CONTRIQUE [65]. Since these image metrics cannot capture distortions in the temporal domain, we also tested several video quality metrics, including FAST [16], SpEED [63], ST-RRED [64], VMAF [15], C3DVQA [17], FRQM [66], ST-GREED [67], VSTR [68] and FloLPIPS [100]. Among these, FAST, SpEED and ST-RRED are conventional metrics that are based on either spatio-temporal gradient information or

³Averaged over three frame rates.

TABLE II

THE PERFORMANCE OF THE TESTED QUALITY METRICS ON THE BVI-VFI DATASET ACROSS DIFFERENT FRAME RATES AND INTERPOLATION METHODS. IN EACH COLUMN, THE BEST AND THE SECOND BEST MODELS ARE **BOLDFACED** AND UNDERLINED.

	30fps		60fps		120fps		non-DL		DL		Overall			
Model	SRCC	PLCC	SRCC	PLCC	SRCC	PLCC	SRCC	PLCC	SRCC	PLCC	SRCC	KRCC	PLCC	RMSE
PSNR	0.38	0.44	<u>0.60</u>	<u>0.55</u>	<u>0.52</u>	0.51	0.35	<u>0.40</u>	<u>0.64</u>	<u>0.64</u>	<u>0.58</u>	<u>0.40</u>	<u>0.53</u>	11.27
SSIM	0.40	0.43	0.59	0.53	0.50	0.46	0.32	0.36	0.61	0.61	0.56	0.38	<u>0.50</u>	11.50
MS-SSIM	0.33	0.39	0.58	0.51	0.51	0.48	0.34	0.37	0.61	0.59	0.56	0.38	0.49	11.57
VIF	0.26	0.28	0.47	0.40	0.41	0.39	0.28	0.34	0.48	0.46	0.45	0.30	0.39	12.28
VSI	0.36	0.41	0.58	0.53	0.51	0.49	0.34	0.37	0.62	0.61	0.57	0.38	0.51	11.42
FSIM	0.36	0.40	0.56	0.51	0.51	0.50	0.34	0.37	0.60	0.59	0.56	0.38	0.50	11.56
GMSD	0.41	0.42	0.57	0.53	0.48	0.48	0.30	0.35	0.61	0.62	0.55	0.37	0.51	11.44
LPIPS	0.29	0.30	0.49	0.46	0.45	0.49	0.31	0.23	0.53	0.53	0.49	0.33	0.45	11.88
DISTS	0.34	0.35	0.49	0.51	0.47	<u>0.57</u>	0.33	0.30	0.56	0.56	0.51	0.35	0.50	11.52
PieAPP	0.32	0.32	0.40	0.40	0.31	0.36	0.23	0.23	0.46	0.45	0.41	0.28	0.39	12.26
deepIQA-FR	0.16	0.23	0.33	0.36	0.27	0.37	0.25	0.26	0.39	0.42	0.36	0.23	0.36	12.42
CONTRIQUE	0.15	0.29	0.19	0.36	0.22	0.42	0.18	0.20	0.36	0.40	0.23	0.15	0.34	12.51
FAST	<u>0.40</u>	0.28	0.67	0.59	0.62	0.66	<u>0.36</u>	0.36	0.72	0.71	0.64	0.45	0.57	10.93
SpEED	0.36	0.00	0.58	0.43	0.50	0.00	0.33	0.20	0.62	0.53	0.57	0.39	0.49	11.56
ST-RRED	0.35	0.00	0.55	0.40	0.47	0.40	0.31	0.30	0.59	0.41	0.54	0.37	0.47	11.77
VMAF	0.36	0.34	0.56	0.50	0.50	0.45	0.31	0.32	0.58	0.57	0.53	0.36	0.47	11.73
C3DVQA	0.15	0.29	0.50	0.42	<u>0.52</u>	0.39	0.29	0.34	0.52	0.45	0.47	0.31	0.40	12.19
FRQM	0.29	0.33	0.52	0.50	<u>0.47</u>	0.51	0.75	0.76	0.46	0.45	0.54	0.37	0.48	11.64
ST-GREED	0.03	0.09	0.05	0.11	0.01	0.22	0.05	0.18	0.04	0.23	0.02	0.01	0.05	13.29
FloLPIPS	0.36	0.38	0.51	0.51	0.49	0.53	<u>0.36</u>	0.26	0.59	0.58	0.54	0.37	<u>0.51</u>	11.45
NIQE	0.32	0.34	0.07	0.21	0.01	0.13	0.04	0.12	0.13	0.29	0.08	0.05	0.18	13.09
deepIQA-NR	0.25	0.25	0.18	0.16	0.15	0.11	0.08	0.13	0.18	0.19	0.16	0.11	0.16	13.14
VIIDEO	0.03	0.09	0.04	0.25	0.15	0.29	0.01	0.09	0.23	0.25	0.09	0.06	0.18	13.09
VIDEVAL	0.18	0.25	0.03	0.12	0.13	0.12	0.13	0.04	0.05	0.09	0.00	0.00	0.05	13.29

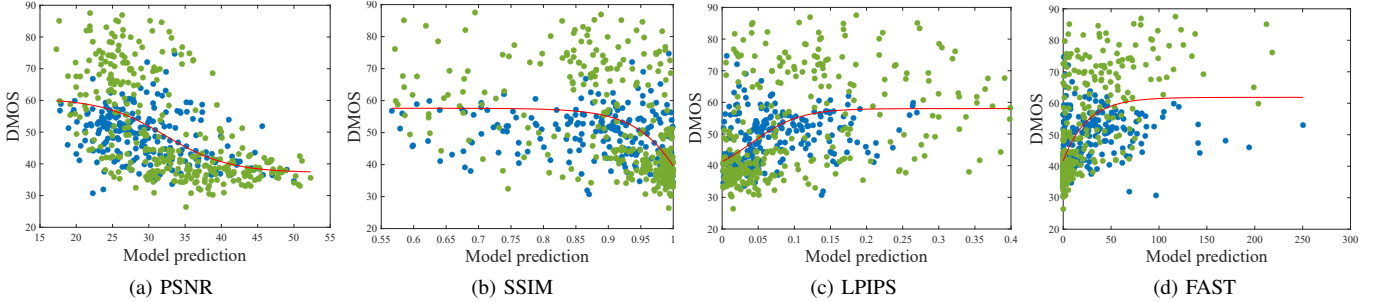


Fig. 6. Scatter plots of DMOS values against the predictions of selected quality models. The blue scatter points correspond to distorted videos generated by non-DL methods, while the green points denote DL-based methods. The red lines are the logistic functions fitted between the model predictions and DMOS values on the entire BVI-VFI database.

natural scene statistics (NSS). VMAF is a popular learning-based metric that uses a support vector regressor (SVR) to combine hand-crafted features. C3DVQA is a deep learning-based metric that processes the reference and distorted videos with a 3D convolutional neural network. FRQM, ST-GREED, and VSTR are specifically designed to capture temporal/spatial resolution-related artefacts. Lastly, FloLPIPS is a recently proposed bespoke metric for VFI that combines distortions in optical flow with LPIPS.

For completeness, we have also considered no-reference (NR) quality metrics. These include image models, NIQE [101] and deepIQA-NR [99], and video models, VIIDEO [102], VBLIINDS [103], VIDEVAL [104], RAPIQUE [105], and FAVER [69].

In order to measure the performance of these quality metrics on predicting subjective quality, we employed four statistical measures: Spearman's Rank-order Correlation Coefficient (SRCC), the Kendall Rank-order Correlation Coefficient (KRCC), Pearson's Linear Correlation Coefficient (PLCC) and Root Mean Squared Error (RMSE). Better prediction

performance is indicated by higher values of the three correlation coefficients and lower RMSE values. For the calculation of PLCC and RMSE, a logistic curve was fit between the ground-truth DMOS values and the metric scores following the procedure in [106].

For all the learning-based metrics (VMAF, ST-GREED, VIDEVAL, C3DVQA), we first generated results based on their publicly available pre-trained models (as shown in Section V-A). However, such pre-trained versions were absent for some of the metrics, including VSTR, FAVER, RAPIQUE, and VBLIINDS. To account for this, and also to allow the models to benefit from their learning-based nature, we also conducted cross-validation experiments (see Section V-B) on the BVI-VFI database. It is noted that the deep learning-based image quality metrics (i.e. LPIPS, DISTS, PieAPP, DeepIQA, CONTRIQUE) were pre-trained on large-scale image quality databases. Since our database only contains ground-truth quality scores at the video level, we did not re-train these models during cross validation.

TABLE III

F-TEST RESULTS BETWEEN DMOS PREDICTION RESIDUALS OF SELECTED QUALITY METRICS AT A 95% CONFIDENCE INTERVAL. THE VALUE “1” INDICATES THE METRIC IN THE ROW IS SUPERIOR TO THE METRIC IN THE COLUMN AND “0” MEANS THE OPPOSITE, WHILE A “-” DENOTES STATISTICAL EQUIVALENCE. IN EACH CELL, THERE ARE 6 ENTRIES CORRESPONDING TO 30FPS, 60FPS, 120FPS, NON-DL, DL AND ALL VIDEOS RESPECTIVELY.

Metric	LPIPS	ST-RRED	FRQM	FloLPIPS	GMSD	FSIM	MS-SSIM	SSIM	SpEED	VSI	PSNR	FAST
LPIPS	-----	-----	---0--	-----	-----	-----	-----	-----	--1---	-----	---0--	--0-00
ST-RRED	-----	-----	---0--	---0--	---0--	---0--	---0--	---0--	-----	---0--	---0--	--0-00
FRQM	---1--	---1--	-----	---10--	---10--	---10--	---10--	---10--	--11--	---10--	---10--	--010-
FloLPIPS	-----	---1-	---01-	-----	-----	-----	-----	-----	--1---	-----	-----	--0-0-
GMSD	-----	---1-	---01-	-----	-----	-----	-----	-----	--1---	-----	-----	--0-0-
FSIM	-----	---1-	---01-	-----	-----	-----	-----	-----	--1---	-----	-----	--0-0-
MS-SSIM	-----	---1-	---01-	-----	-----	-----	-----	-----	--1---	-----	-----	--0-0-
SSIM	-----	---1-	---01-	-----	-----	-----	-----	-----	-----	-----	-----	--0-0-
SpEED	--0---	-----	--00--	--0---	--0---	--0---	--0---	-----	-----	--0---	--0-0-	--0-0-
VSI	-----	---1-	---01-	-----	-----	-----	-----	-----	--1---	-----	-----	--0-0-
PSNR	---1-	---1-	---01-	-----	-----	-----	-----	-----	--1-1-	-----	-----	--0-0-
FAST	--1-11	-11-11	--101-	--1-1-	--1-1-	--1-1-	--1-1-	--1-1-	--1-1-	--1-1-	--1-1-	-----

A. Overall Performance on BVI-VFI

We first evaluate the overall performance of all the tested quality assessment methods (except for VSTR, FAVER, RAPIQUE and VBLINDS, as explained above) on the entire BVI-VFI database. Table II summarises these results as well as the performance at the three specific frame rates. It can be observed that none of the tested metrics exhibit satisfactory overall correlation with the subjective quality scores, with the best-performing metric, FAST, achieving a SRCC value of only 0.64. This may be due to the approach employed in FAST, which captures spatio-temporal quality degradation by comparing the moving parts of the reference and distorted frames along motion trajectories. It can also be seen that the metrics most commonly used in the VFI literature (PSNR, SSIM and LPIPS) all achieved SRCC values below 0.6. This indicates that there is still significant scope for improving the accuracy of quality metrics in the context of VFI. The last four rows of Table II report the performance of four no-reference quality assessment models. These methods significantly underperformed most of the full-/reduced-reference models.

When comparing the variation of model performance across different frame rates (Table II), it can be seen that most models achieved highest correlation with opinion scores on videos at 60fps and the lowest correlation on 30fps sequences. This implies that these models could not properly account for the effect of frame rate on the human perception of interpolation artefacts, and that frame rate can be a useful factor to consider when designing a better quality assessment model for frame interpolated content.

Table II also presents the evaluation results for different VFI algorithms: non-deep learning-based (non-DL) or deep learning-based (DL). It can be observed that the wavelet-based VQA model FRQM achieved the highest SRCC value of 0.75 on sequences interpolated by non-DL methods, but its performance on DL-based group dropped significantly. Similarly, FAST, which achieved the highest SRCC value (of 0.72) on the DL group, saw a large performance degradation on the sequences in the non-DL group. This indicates that if only DL-based VFI methods are concerned, FAST is a more reliable quality metric for evaluating the perceptual quality of VFI content. The scatter plots of the model predictions and DMOS values, as well as the fitted logistic curves, are shown

in Fig. 6 for FAST and the three most popular metrics in VFI: PSNR, SSIM and LPIPS.

To confirm the statistical significance of difference between model performances, we also conducted F-tests among eleven metrics with the best overall SRCC values, plus the widely employed LPIPS. For every pair of quality metrics, the F-test was performed on the residuals between the ground-truth DMOS values and the DMOS predicted by those metrics through the fitted logistic curves [84, 86]. Assuming that the residuals follow a zero-mean Gaussian distribution, the F-test is under the null hypothesis that two groups of residuals have equal variance at 95% confidence level. Table III summarises the F-test results, where it can be seen that FAST outperformed all the other eleven models significantly on videos in the DL group. FRQM also offers a significantly better performance over other tested metrics for the non-DL group. This further confirms the findings we described above.

B. Cross-Validation Results for Learning-based Models

As mentioned above, for some learning-based metrics, we also conducted cross-validation experiments where the models were trained and evaluated on randomly split non-overlapping data sets. Specifically, we performed five-fold cross validation as in [86], where 80% of the 540 distorted videos are used as the training set and the other 20% as the test set. To better evaluate the generalisation ability of the learning-based metrics, we ensured the content-wise separation between the training and test sets, i.e. the source contents of all the training videos are distinct from those of the test videos. As a result, 435 distorted videos from 29 sources were in the training set, and the other 105 distorted videos from 7 sources fell in the test set. In each of such splits, we trained each of the learning-based models following their original training method and evaluated them on the test set. For those metrics that do not need re-training, we simply tested them on the test set. Such random training-test data splitting was repeated 1000 times, and the medians and standard deviations of the SRCC and PLCC values were calculated and reported in Table IV.

We can observe from Table IV that FAST remained the best-performing metric in terms of SRCC, whereas the learning-based method ST-GREED ranked top in terms of PLCC. This implies the effectiveness of the entropic difference features

TABLE IV

CROSS VALIDATION RESULTS OF THE TESTED QUALITY ASSESSMENT METHODS ON THE BVI-VFI DATASET ACROSS DIFFERENT FRAME RATES AND INTERPOLATION METHODS. EACH CELL PRESENTS THE MEDIAN AND STANDARD DEVIATION OF THE STATISTICAL MEASURES OBTAINED OVER 1000 RANDOM TRAIN-TEST SPLITS. IN EACH COLUMN, THE BEST AND THE SECOND BEST MODELS ARE **BOLDFACED** AND UNDERLINED.

	30fps		60fps		120fps		non-DL		DL		Overall	
Model	SRCC	PLCC	SRCC	PLCC	SRCC	PLCC	SRCC	PLCC	SRCC	PLCC	SRCC	PLCC
PSNR	0.43 (0.14)	0.55 (0.14)	0.62 (0.12)	0.62 (0.10)	0.52 (0.17)	0.59 (0.14)	0.37 (0.13)	0.46 (0.12)	0.65 (0.09)	0.68 (0.09)	0.60 (0.08)	0.57 (0.08)
SSIM	0.45 (0.14)	0.58 (0.14)	0.62 (0.12)	0.61 (0.10)	0.51 (0.19)	0.57 (0.14)	0.37 (0.12)	0.45 (0.13)	0.63 (0.10)	0.67 (0.10)	0.58 (0.09)	0.56 (0.08)
MS-SSIM	0.39 (0.15)	0.55 (0.15)	0.61 (0.11)	0.59 (0.10)	0.51 (0.18)	0.59 (0.14)	0.38 (0.12)	0.45 (0.13)	0.62 (0.09)	0.65 (0.09)	0.58 (0.08)	0.55 (0.08)
VIF	0.30 (0.14)	0.44 (0.15)	0.50 (0.12)	0.50 (0.12)	0.42 (0.18)	0.52 (0.14)	0.31 (0.12)	0.40 (0.11)	0.51 (0.10)	0.54 (0.11)	0.48 (0.09)	0.45 (0.09)
VSI	0.40 (0.15)	<u>0.56 (0.15)</u>	0.60 (0.12)	0.60 (0.10)	0.52 (0.17)	0.60 (0.13)	0.38 (0.12)	0.45 (0.11)	0.63 (0.09)	0.66 (0.09)	0.58 (0.09)	0.56 (0.08)
FSIM	0.40 (0.14)	<u>0.55 (0.14)</u>	0.58 (0.12)	0.59 (0.10)	0.52 (0.17)	0.61 (0.14)	0.38 (0.11)	0.45 (0.11)	0.62 (0.09)	0.65 (0.09)	0.58 (0.08)	0.55 (0.08)
GMSD	0.45 (0.15)	0.56 (0.14)	0.59 (0.13)	0.60 (0.10)	0.49 (0.18)	0.59 (0.13)	0.34 (0.13)	0.43 (0.13)	0.62 (0.10)	0.67 (0.10)	0.57 (0.09)	0.57 (0.09)
LPIPS	0.33 (0.14)	<u>0.47 (0.15)</u>	0.50 (0.13)	0.54 (0.13)	0.45 (0.17)	0.59 (0.16)	0.36 (0.12)	0.38 (0.17)	0.54 (0.09)	0.58 (0.10)	0.51 (0.09)	0.51 (0.10)
DISTS	0.36 (0.14)	0.45 (0.14)	0.49 (0.10)	0.57 (0.10)	0.48 (0.15)	0.65 (0.12)	0.35 (0.09)	0.38 (0.13)	0.56 (0.08)	0.61 (0.09)	0.52 (0.07)	0.54 (0.08)
PieAPP	0.34 (0.17)	0.45 (0.14)	0.41 (0.15)	0.49 (0.13)	0.32 (0.19)	0.48 (0.15)	0.25 (0.13)	0.34 (0.12)	0.46 (0.13)	0.53 (0.12)	0.42 (0.12)	0.45 (0.11)
deepIQA-FR	0.18 (0.16)	0.35 (0.15)	0.34 (0.16)	0.44 (0.12)	0.26 (0.19)	0.43 (0.15)	0.28 (0.13)	0.37 (0.12)	0.38 (0.13)	0.47 (0.12)	0.36 (0.12)	0.41 (0.10)
CONTRIQUE	0.14 (0.10)	0.33 (0.12)	0.17 (0.10)	0.42 (0.11)	0.21 (0.13)	0.48 (0.12)	0.18 (0.09)	0.26 (0.11)	0.34 (0.10)	0.45 (0.09)	0.22 (0.07)	0.37 (0.08)
FAST	0.43 (0.15)	0.56 (0.18)	0.68 (0.11)	0.65 (0.16)	0.62 (0.17)	0.75 (0.19)	0.40 (0.12)	0.41 (0.14)	0.73 (0.08)	0.74 (0.09)	0.66 (0.09)	0.61 (0.10)
SpEED	0.40 (0.17)	0.26 (0.16)	0.60 (0.12)	0.44 (0.20)	0.50 (0.17)	0.44 (0.18)	0.36 (0.12)	0.19 (0.13)	0.63 (0.09)	0.54 (0.13)	0.58 (0.09)	0.43 (0.12)
ST-RRED	0.39 (0.15)	0.26 (0.18)	0.57 (0.12)	0.42 (0.20)	0.47 (0.17)	0.40 (0.19)	0.33 (0.12)	0.19 (0.13)	0.61 (0.09)	0.53 (0.14)	0.55 (0.09)	0.41 (0.12)
VMAF	0.36 (0.17)	0.49 (0.14)	0.52 (0.13)	0.52 (0.11)	0.41 (0.18)	0.54 (0.16)	0.29 (0.13)	0.38 (0.12)	0.56 (0.11)	0.58 (0.11)	0.47 (0.11)	0.46 (0.10)
C3DVQA	0.34 (0.14)	0.32 (0.12)	0.45 (0.08)	0.52 (0.02)	0.28 (0.17)	0.30 (0.12)	0.22 (0.09)	0.40 (0.06)	0.53 (0.09)	0.57 (0.03)	0.43 (0.05)	0.42 (0.06)
FRQM	0.31 (0.18)	0.46 (0.16)	0.55 (0.13)	0.57 (0.11)	0.48 (0.18)	0.57 (0.15)	0.76 (0.07)	0.79 (0.07)	0.46 (0.07)	0.46 (0.07)	0.54 (0.06)	0.49 (0.06)
ST-GREED	0.45 (0.15)	0.53 (0.13)	0.69 (0.11)	0.70 (0.11)	0.55 (0.18)	<u>0.70 (0.16)</u>	0.36 (0.12)	0.42 (0.12)	0.71 (0.09)	0.75 (0.09)	0.64 (0.09)	0.64 (0.10)
FloLPIPS	0.38 (0.16)	0.52 (0.16)	0.52 (0.13)	0.57 (0.12)	0.48 (0.16)	0.64 (0.15)	0.40 (0.12)	0.44 (0.18)	0.60 (0.09)	0.62 (0.09)	0.56 (0.09)	0.56 (0.10)
VSTR	0.40 (0.16)	0.49 (0.14)	0.62 (0.11)	0.64 (0.11)	0.45 (0.17)	0.63 (0.17)	0.36 (0.13)	0.41 (0.12)	0.64 (0.10)	0.68 (0.10)	0.58 (0.10)	0.57 (0.10)
NIQE	0.35 (0.11)	0.40 (0.11)	0.13 (0.14)	0.28 (0.10)	0.07 (0.19)	0.25 (0.09)	0.10 (0.09)	0.24 (0.09)	0.18 (0.11)	0.34 (0.11)	0.12 (0.08)	0.23 (0.09)
deepIQA-NR	0.29 (0.10)	0.33 (0.09)	0.21 (0.14)	0.28 (0.10)	0.18 (0.17)	0.23 (0.11)	0.10 (0.08)	0.22 (0.09)	0.22 (0.10)	0.30 (0.11)	0.18 (0.08)	0.23 (0.08)
VVIDEO	0.04 (0.13)	0.25 (0.12)	0.03 (0.12)	0.32 (0.14)	0.14 (0.13)	0.34 (0.13)	0.05 (0.04)	0.17 (0.10)	0.22 (0.13)	0.32 (0.12)	0.09 (0.07)	0.26 (0.10)
VIDEVAL	0.42 (0.14)	0.48 (0.12)	0.37 (0.13)	0.43 (0.12)	0.34 (0.19)	0.55 (0.16)	0.26 (0.14)	0.35 (0.13)	0.40 (0.15)	0.50 (0.13)	0.34 (0.12)	0.40 (0.11)
RAPIQUE	0.09 (0.16)	0.12 (0.18)	0.35 (0.14)	0.44 (0.14)	0.37 (0.15)	0.47 (0.19)	0.21 (0.14)	0.24 (0.15)	0.33 (0.12)	0.41 (0.13)	0.27 (0.12)	0.36 (0.11)
VBLINDS	0.43 (0.13)	0.50 (0.11)	0.52 (0.13)	0.59 (0.13)	0.30 (0.19)	0.56 (0.18)	0.25 (0.12)	0.32 (0.11)	0.52 (0.14)	0.57 (0.13)	0.38 (0.12)	0.42 (0.12)
FAVER	0.47 (0.14)	0.52 (0.12)	0.36 (0.14)	0.45 (0.14)	0.26 (0.18)	0.46 (0.19)	<u>0.53 (0.13)</u>	<u>0.58 (0.12)</u>	0.47 (0.15)	0.54 (0.13)	0.45 (0.12)	0.49 (0.11)

extracted in ST-GREED in capturing temporal artefacts. It is also noticeable that the learning-based no-reference model FAVER, which is designed to predict the quality of variable-frame rate videos, also achieved competitive performance compared to some of the full-reference models. The cross-validation results for different types of VFI algorithms are also presented in Table IV, which shows that on DL-interpolated videos, FAST and ST-GREED achieved higher correlation compared to all the other models, while FRQM and FAVER outperforms others for the non-NL group.

C. Summary

From the evaluation results presented above, we observed that firstly, none of the 28 tested quality models showed consistent performance across different frame rates. This indicates that consideration should be taken on how humans perceive the interpolation artefacts at different frame rates. Secondly, the evaluated metrics were also not robust against various types of interpolation algorithms, with most models except FRQM performing better on sequences interpolated by DL-based VFI methods. Finally, our results showed that the motion saliency-based full reference VQA model, FAST, achieved the best overall performance on predicting the perceptual quality of interpolated videos, in particular on those interpolated by DL-based VFI methods. However, the overall SRCC value achieved by FAST was 0.64, which is far from satisfactory. Therefore, a much more accurate quality metric is urgently needed which can better predict the perceptual quality of interpolated videos.

VI. CONCLUSION AND FUTURE WORK

In this paper, we presented a video quality database, BVI-VFI, which was employed to perform a subjective study on

the perceptual quality of video frame interpolated content. The database comprises 108 reference and 540 distorted sequences with frame rates of 30, 60 and 120 fps. The distorted sequences were generated from 36 diverse source sequences at three spatial resolutions using five representative video frame interpolation methods. Based upon this database, we conducted a large scale psychophysical experiment to collect more than 10800 subjective opinion scores from 189 participants. The collected subjective data shows that the state-of-the-art deep learning (DL)-based VFI algorithms achieve better overall interpolation performance over simple frame averaging and repeating, in particular when the frame rate is low. As the frame rate increases, this improvement becomes less evident.

Using this database, we have also benchmarked the performance of 28 image/video quality assessment metrics. The results indicate that all the three commonly used quality metrics for VFI, PSNR, SSIM and LPIPS, achieve poor correlation with subjective opinions scores on this database. Even the best-performing metric, FAST, was unsatisfactory with an overall SRCC value of only 0.64. This clearly highlights the urgent need for a new quality metric capable of accurately predicting the perceptual quality of VFI content.

To the best of our knowledge, BVI-VFI is the first video quality database that contains purely VFI-induced artefacts, which allows us to thoroughly study the subjective quality of frame interpolated content and measure the performance of existing video quality metrics on assessing VFI quality. It provides a valuable resource for developing and validating new perceptual quality metrics for VFI, and it can be also employed to evaluate the performance of VFI algorithms.

REFERENCES

- [1] H. Jiang, D. Sun, V. Jampani, M.-H. Yang, E. Learned-Miller, and J. Kautz, "Super slo-mo: High quality estimation of multiple inter-

- mediate frames for video interpolation,” in *Proceedings of the IEEE Conference on Computer Vision and Pattern Recognition*, 2018, pp. 9000–9008.
- [2] M. Usman, X. He, K.-M. Lam, M. Xu, S. M. M. Bokhari, and J. Chen, “Frame interpolation for cloud-based mobile video streaming,” *IEEE Transactions on Multimedia*, vol. 18, no. 5, pp. 831–839, 2016.
 - [3] N. Karani, C. Tanner, S. Kozierke, and E. Konukoglu, “Temporal interpolation of abdominal mris acquired during free-breathing,” in *International Conference on Medical Image Computing and Computer-Assisted Intervention*. Springer, 2017, pp. 359–367.
 - [4] L. Siyao, S. Zhao, W. Yu, W. Sun, D. Metaxas, C. C. Loy, and Z. Liu, “Deep animation video interpolation in the wild,” in *Proceedings of the IEEE/CVF Conference on Computer Vision and Pattern Recognition*, 2021, pp. 6587–6595.
 - [5] X. Xu, L. Siyao, W. Sun, Q. Yin, and M.-H. Yang, “Quadratic video interpolation,” in *NeurIPS*, 2019.
 - [6] D. Danier, F. Zhang, and D. Bull, “ST-MFNet: A spatio-temporal multi-flow network for frame interpolation,” in *Proceedings of the IEEE/CVF Conference on Computer Vision and Pattern Recognition*, 2022, pp. 3521–3531.
 - [7] L. Lu, R. Wu, H. Lin, J. Lu, and J. Jia, “Video frame interpolation with transformer,” in *Proceedings of the IEEE/CVF Conference on Computer Vision and Pattern Recognition*, 2022, pp. 3532–3542.
 - [8] D. M. Argaw and I. S. Kweon, “Long-term video frame interpolation via feature propagation,” in *Proceedings of the IEEE/CVF Conference on Computer Vision and Pattern Recognition*, 2022, pp. 3543–3552.
 - [9] P. Hu, S. Niklaus, S. Sclaroff, and K. Saenko, “Many-to-many splatting for efficient video frame interpolation,” in *Proceedings of the IEEE/CVF Conference on Computer Vision and Pattern Recognition*, 2022, pp. 3553–3562.
 - [10] M. Liu, C. Xu, C. Yao, C. Lin, and Y. Zhao, “JNMR: Joint non-linear motion regression for video frame interpolation,” *arXiv preprint arXiv:2206.04231*, 2022.
 - [11] Z. Wang, A. C. Bovik, H. R. Sheikh, and E. P. Simoncelli, “Image quality assessment: from error visibility to structural similarity,” *IEEE transactions on image processing*, vol. 13, no. 4, pp. 600–612, 2004.
 - [12] R. Zhang, P. Isola, A. A. Efros, E. Shechtman, and O. Wang, “The unreasonable effectiveness of deep features as a perceptual metric,” in *Proceedings of the IEEE conference on computer vision and pattern recognition*, 2018, pp. 586–595.
 - [13] L. Zhang, Y. Shen, and H. Li, “VSI: A visual saliency-induced index for perceptual image quality assessment,” *IEEE Transactions on Image processing*, vol. 23, no. 10, pp. 4270–4281, 2014.
 - [14] K. Ding, K. Ma, S. Wang, and E. P. Simoncelli, “Image quality assessment: Unifying structure and texture similarity,” *IEEE transactions on pattern analysis and machine intelligence*, 2020.
 - [15] Z. Li, A. Aaron, I. Katsavounidis, A. Moorthy, and M. Manohara, “Toward a practical perceptual video quality metric,” *The Netflix Tech Blog*, vol. 6, no. 2, 2016.
 - [16] J. Wu, Y. Liu, W. Dong, G. Shi, and W. Lin, “Quality assessment for video with degradation along salient trajectories,” *IEEE Transactions on Multimedia*, vol. 21, no. 11, pp. 2738–2749, 2019.
 - [17] M. Xu, J. Chen, H. Wang, S. Liu, G. Li, and Z. Bai, “C3DVQA: Full-reference video quality assessment with 3d convolutional neural network,” in *ICASSP 2020-2020 IEEE International Conference on Acoustics, Speech and Signal Processing (ICASSP)*. IEEE, 2020, pp. 4447–4451.
 - [18] T. Kalluri, D. Pathak, M. Chandraker, and D. Tran, “FLAVR: Flow-agnostic video representations for fast frame interpolation,” *arXiv preprint arXiv:2012.08512*, 2020.
 - [19] H. Men, H. Lin, V. Hosu, D. Maurer, A. Bruhn, and D. Saupe, “Visual quality assessment for motion compensated frame interpolation,” in *2019 Eleventh International Conference on Quality of Multimedia Experience (QoMEX)*. IEEE, 2019, pp. 1–6.
 - [20] H. Men, V. Hosu, H. Lin, A. Bruhn, and D. Saupe, “Visual quality assessment for interpolated slow-motion videos based on a novel database,” in *2020 Twelfth International Conference on Quality of Multimedia Experience (QoMEX)*. IEEE, 2020, pp. 1–6.
 - [21] D. Danier, F. Zhang, and D. Bull, “A subjective quality study for video frame interpolation,” *arXiv preprint arXiv:2202.07727*, 2022.
 - [22] J. L. Barron, D. J. Fleet, and S. S. Beauchemin, “Performance of optical flow techniques,” *International journal of computer vision*, vol. 12, no. 1, pp. 43–77, 1994.
 - [23] S. Baker, D. Scharstein, J. Lewis, S. Roth, M. J. Black, and R. Szeliski, “A database and evaluation methodology for optical flow,” *International journal of computer vision*, vol. 92, no. 1, pp. 1–31, 2011.
 - [24] J. Park, K. Ko, C. Lee, and C.-S. Kim, “BMBC: Bilateral motion estimation with bilateral cost volume for video interpolation,” in *Computer Vision—ECCV 2020: 16th European Conference, Glasgow, UK, August 23–28, 2020, Proceedings, Part XIV 16*. Springer, 2020, pp. 109–125.
 - [25] S. Niklaus and F. Liu, “Context-aware synthesis for video frame interpolation,” in *Proceedings of the IEEE conference on computer vision and pattern recognition*, 2018, pp. 1701–1710.
 - [26] Z. Liu, R. A. Yeh, X. Tang, Y. Liu, and A. Agarwala, “Video frame synthesis using deep voxel flow,” in *Proceedings of the IEEE International Conference on Computer Vision*, 2017, pp. 4463–4471.
 - [27] T. Xue, B. Chen, J. Wu, D. Wei, and W. T. Freeman, “Video enhancement with task-oriented flow,” *International Journal of Computer Vision*, vol. 127, no. 8, pp. 1106–1125, 2019.
 - [28] Z. Huang, T. Zhang, W. Heng, B. Shi, and S. Zhou, “RIFE: Real-time intermediate flow estimation for video frame interpolation,” *arXiv preprint arXiv:2011.06294*, 2020.
 - [29] J. Park, C. Lee, and C.-S. Kim, “Asymmetric bilateral motion estimation for video frame interpolation,” in *International Conference on Computer Vision*, 2021.
 - [30] H. Zhang, Y. Zhao, and R. Wang, “A flexible recurrent residual pyramid network for video frame interpolation,” in *European Conference on Computer Vision*. Springer, 2020, pp. 474–491.
 - [31] H. Sim, J. Oh, and M. Kim, “XVFI: extreme video frame interpolation,” in *Proceedings of the IEEE International Conference on Computer Vision (ICCV)*, 2021.
 - [32] L. Kong, B. Jiang, D. Luo, W. Chu, X. Huang, Y. Tai, C. Wang, and J. Yang, “IFRNet: Intermediate feature refine network for efficient frame interpolation,” in *Proceedings of the IEEE/CVF Conference on Computer Vision and Pattern Recognition*, 2022, pp. 1969–1978.
 - [33] F. Reda, J. Kontkanen, E. Tabellion, D. Sun, C. Pantofaru, and B. Curless, “FILM: Frame interpolation for large motion,” *arXiv preprint arXiv:2202.04901*, 2022.
 - [34] S. Niklaus and F. Liu, “Softmax splatting for video frame interpolation,” in *Proceedings of the IEEE/CVF Conference on Computer Vision and Pattern Recognition*, 2020, pp. 5437–5446.
 - [35] S. Niklaus, P. Hu, and J. Chen, “Splatting-based synthesis for video frame interpolation,” *arXiv preprint arXiv:2201.10075*, 2022.
 - [36] Y. Liu, L. Xie, L. Siyao, W. Sun, Y. Qiao, and C. Dong, “Enhanced quadratic video interpolation,” in *European Conference on Computer Vision*. Springer, 2020, pp. 41–56.
 - [37] S. Niklaus, L. Mai, and F. Liu, “Video frame interpolation via adaptive convolution,” in *Proceedings of the IEEE Conference on Computer Vision and Pattern Recognition*, 2017, pp. 670–679.
 - [38] —, “Video frame interpolation via adaptive separable convolution,” in *Proceedings of the IEEE International Conference on Computer Vision*, 2017, pp. 261–270.
 - [39] H. Lee, T. Kim, T.-y. Chung, D. Pak, Y. Ban, and S. Lee, “AdaCoF: Adaptive collaboration of flows for video frame interpolation,” in *Proceedings of the IEEE/CVF Conference on Computer Vision and Pattern Recognition*, 2020, pp. 5316–5325.
 - [40] S. Gui, C. Wang, Q. Chen, and D. Tao, “FeatureFlow: Robust video interpolation via structure-to-texture generation,” in *Proceedings of the IEEE/CVF Conference on Computer Vision and Pattern Recognition*, 2020, pp. 14 004–14 013.
 - [41] Z. Shi, X. Liu, K. Shi, L. Dai, and J. Chen, “Video interpolation via generalized deformable convolution,” *arXiv e-prints*, pp. arXiv–2008, 2020.
 - [42] T. Ding, L. Liang, Z. Zhu, and I. Zharkov, “CDFI: Compression-driven network design for frame interpolation,” in *Proceedings of the IEEE/CVF Conference on Computer Vision and Pattern Recognition*, 2021, pp. 8001–8011.
 - [43] X. Cheng and Z. Chen, “Multiple video frame interpolation via enhanced deformable separable convolution,” *IEEE Transactions on Pattern Analysis and Machine Intelligence*, 2021.
 - [44] Z. Chen, R. Wang, H. Liu, and Y. Wang, “PDWN: Pyramid deformable warping network for video interpolation,” *IEEE Open Journal of Signal Processing*, pp. 1–1, 2021.
 - [45] D. Danier, F. Zhang, and D. Bull, “Enhancing deformable convolution based video frame interpolation with coarse-to-fine 3d cnn,” *arXiv preprint arXiv:2202.07731*, 2022.
 - [46] Z. Shi, X. Xu, X. Liu, J. Chen, and M.-H. Yang, “Video frame interpolation transformer,” in *Proceedings of the IEEE/CVF Conference on Computer Vision and Pattern Recognition*, 2022, pp. 17 482–17 491.
 - [47] J. Dai, H. Qi, Y. Xiong, Y. Li, G. Zhang, H. Hu, and Y. Wei, “Deformable convolutional networks,” in *Proceedings of the IEEE international conference on computer vision*, 2017, pp. 764–773.
 - [48] W. Bao, W.-S. Lai, C. Ma, X. Zhang, Z. Gao, and M.-H. Yang, “Depth-

- aware video frame interpolation,” in *Proceedings of the IEEE/CVF Conference on Computer Vision and Pattern Recognition*, 2019, pp. 3703–3712.
- [49] W. Bao, W.-S. Lai, X. Zhang, Z. Gao, and M.-H. Yang, “MEMC-Net: Motion estimation and motion compensation driven neural network for video interpolation and enhancement,” *IEEE transactions on pattern analysis and machine intelligence*, 2019.
- [50] M. Choi, H. Kim, B. Han, N. Xu, and K. M. Lee, “Channel attention is all you need for video frame interpolation,” in *Proceedings of the AAAI Conference on Artificial Intelligence*, vol. 34, 2020, pp. 10663–10671.
- [51] S. Meyer, O. Wang, H. Zimmer, M. Grosse, and A. Sorkine-Hornung, “Phase-based frame interpolation for video,” in *Proceedings of the IEEE conference on computer vision and pattern recognition*, 2015, pp. 1410–1418.
- [52] S. Meyer, A. Djelouah, B. McWilliams, A. Sorkine-Hornung, M. Gross, and C. Schroers, “Phasenet for video frame interpolation,” in *Proceedings of the IEEE Conference on Computer Vision and Pattern Recognition*, 2018, pp. 498–507.
- [53] S. Tulyakov, D. Gehrig, S. Georgoulis, J. Erbach, M. Gehrig, Y. Li, and D. Scaramuzza, “Time Lens: Event-based video frame interpolation,” in *Proceedings of the IEEE/CVF Conference on Computer Vision and Pattern Recognition*, 2021, pp. 16155–16164.
- [54] S. Tulyakov, A. Bochicchio, D. Gehrig, S. Georgoulis, Y. Li, and D. Scaramuzza, “Time Lens++: Event-based frame interpolation with parametric non-linear flow and multi-scale fusion,” in *Proceedings of the IEEE/CVF Conference on Computer Vision and Pattern Recognition*, 2022, pp. 17755–17764.
- [55] W. He, K. You, Z. Qiao, X. Jia, Z. Zhang, W. Wang, H. Lu, Y. Wang, and J. Liao, “TimeReplayer: Unlocking the potential of event cameras for video interpolation,” in *Proceedings of the IEEE/CVF Conference on Computer Vision and Pattern Recognition*, 2022, pp. 17804–17813.
- [56] F. A. Reda, D. Sun, A. Dundar, M. Shoeybi, G. Liu, K. J. Shih, A. Tao, J. Kautz, and B. Catanzaro, “Unsupervised video interpolation using cycle consistency,” in *Proceedings of the IEEE/CVF International Conference on Computer Vision*, 2019, pp. 892–900.
- [57] Z. Cheng, S. Jiang, and H. Li, “Unsupervised video interpolation by learning multilayered 2.5 d motion fields,” *arXiv preprint arXiv:2204.09900*, 2022.
- [58] M. Choi, J. Choi, S. Baik, T. H. Kim, and K. M. Lee, “Test-time adaptation for video frame interpolation via meta-learning,” *IEEE Transactions on Pattern Analysis and Machine Intelligence*, pp. 1–1, 2021.
- [59] W. Shen, W. Bao, G. Zhai, L. Chen, X. Min, and Z. Gao, “Blurry video frame interpolation,” in *Proceedings of the IEEE/CVF conference on computer vision and pattern recognition*, 2020, pp. 5114–5123.
- [60] Y. Zhang, C. Wang, and D. Tao, “Video frame interpolation without temporal priors,” *Advances in Neural Information Processing Systems*, vol. 33, pp. 13308–13318, 2020.
- [61] Z. Wang, E. P. Simoncelli, and A. C. Bovik, “Multiscale structural similarity for image quality assessment,” in *The Thirty-Seventh Asilomar Conference on Signals, Systems & Computers*, 2003, vol. 2. Ieee, 2003, pp. 1398–1402.
- [62] H. R. Sheikh, A. C. Bovik, and G. De Veciana, “An information fidelity criterion for image quality assessment using natural scene statistics,” *IEEE Transactions on image processing*, vol. 14, no. 12, pp. 2117–2128, 2005.
- [63] C. G. Bampis, P. Gupta, R. Soundararajan, and A. C. Bovik, “SpEED-QA: Spatial efficient entropic differencing for image and video quality,” *IEEE signal processing letters*, vol. 24, no. 9, pp. 1333–1337, 2017.
- [64] R. Soundararajan and A. C. Bovik, “Video quality assessment by reduced reference spatio-temporal entropic differencing,” *IEEE Transactions on Circuits and Systems for Video Technology*, vol. 23, no. 4, pp. 684–694, 2012.
- [65] P. C. Madhusudana, N. Birkbeck, Y. Wang, B. Adsumilli, and A. C. Bovik, “Image quality assessment using contrastive learning,” *IEEE Transactions on Image Processing*, vol. 31, pp. 4149–4161, 2022.
- [66] F. Zhang, A. Mackin, and D. R. Bull, “A frame rate dependent video quality metric based on temporal wavelet decomposition and spatiotemporal pooling,” in *2017 IEEE International Conference on Image Processing (ICIP)*. IEEE, 2017, pp. 300–304.
- [67] P. C. Madhusudana, N. Birkbeck, Y. Wang, B. Adsumilli, and A. C. Bovik, “ST-GREED: Space-time generalized entropic differences for frame rate dependent video quality prediction,” *IEEE Transactions on Image Processing*, vol. 30, pp. 7446–7457, 2021.
- [68] D. Y. Lee, H. Ko, J. Kim, and A. C. Bovik, “Space-time video regularity and visual fidelity: Compression, resolution and frame rate adaptation,” *arXiv preprint arXiv:2103.16771*, 2021.
- [69] Q. Zheng, Z. Tu, P. C. Madhusudana, X. Zeng, A. C. Bovik, and Y. Fan, “FAVER: Blind quality prediction of variable frame rate videos,” *arXiv preprint arXiv:2201.01492*, 2022.
- [70] J. Antkowiak, T. Jamal Baina, F. V. Baroncini, N. Chateau, F. FranceT-elecom, A. C. F. Pessoa, F. Stephanie Colonnese, I. L. Contin, J. Caviedes, and F. Philips, “Final report from the video quality experts group on the validation of objective models of video quality assessment march 2000,” 2000.
- [71] K. Seshadrinathan, R. Soundararajan, A. C. Bovik, and L. K. Cormack, “Study of subjective and objective quality assessment of video,” *IEEE transactions on Image Processing*, vol. 19, no. 6, pp. 1427–1441, 2010.
- [72] A. K. Moorthy, L. K. Choi, A. C. Bovik, and G. De Veciana, “Video quality assessment on mobile devices: Subjective, behavioral and objective studies,” *IEEE Journal of Selected Topics in Signal Processing*, vol. 6, no. 6, pp. 652–671, 2012.
- [73] P. V. Vu and D. M. Chandler, “ViS3: An algorithm for video quality assessment via analysis of spatial and spatiotemporal slices,” *Journal of Electronic Imaging*, vol. 23, no. 1, p. 013016, 2014.
- [74] F. Zhang, F. M. Moss, R. Baddeley, and D. R. Bull, “BVI-HD: A video quality database for hevc compressed and texture synthesized content,” *IEEE Transactions on Multimedia*, vol. 20, no. 10, pp. 2620–2630, 2018.
- [75] X. Min, G. Zhai, J. Zhou, M. C. Farias, and A. C. Bovik, “Study of subjective and objective quality assessment of audio-visual signals,” *IEEE Transactions on Image Processing*, vol. 29, pp. 6054–6068, 2020.
- [76] S. Wen, S. Ling, J. Wang, X. Chen, Y. Jing, and P. L. Callet, “Subjective and objective quality assessment of mobile gaming video,” in *ICASSP 2022 - 2022 IEEE International Conference on Acoustics, Speech and Signal Processing (ICASSP)*, 2022, pp. 1810–1814.
- [77] T. Li, X. Min, H. Zhao, G. Zhai, Y. Xu, and W. Zhang, “Subjective and objective quality assessment of compressed screen content videos,” *IEEE Transactions on Broadcasting*, vol. 67, no. 2, pp. 438–449, 2020.
- [78] Z. Shang, J. P. Ebenezer, Y. Wu, H. Wei, S. Sethuraman, and A. C. Bovik, “Study of the subjective and objective quality of high motion live streaming videos,” *IEEE Transactions on Image Processing*, vol. 31, pp. 1027–1041, 2021.
- [79] J. Y. Lin, R. Song, C.-H. Wu, T. Liu, H. Wang, and C.-C. J. Kuo, “MCL-V: A streaming video quality assessment database,” *Journal of Visual Communication and Image Representation*, vol. 30, pp. 1–9, 2015.
- [80] M. Cheon and J.-S. Lee, “Subjective and objective quality assessment of compressed 4k uhd videos for immersive experience,” *IEEE Transactions on Circuits and Systems for Video Technology*, vol. 28, no. 7, pp. 1467–1480, 2017.
- [81] A. Mackin, F. Zhang, and D. R. Bull, “A study of high frame rate video formats,” *IEEE Transactions on Multimedia*, vol. 21, no. 6, pp. 1499–1512, 2018.
- [82] A. Mackin, D. Ma, F. Zhang, and D. Bull, “A subjective study on videos at various bit depths,” in *2021 Picture Coding Symposium (PCS)*. IEEE, 2021, pp. 1–5.
- [83] Q. Huang, S. Y. Jeong, S. Yang, D. Zhang, S. Hu, H. Y. Kim, J. S. Choi, and C.-C. J. Kuo, “Perceptual quality driven frame-rate selection (pqd-frs) for high-frame-rate video,” *IEEE Transactions on Broadcasting*, vol. 62, no. 3, pp. 640–653, 2016.
- [84] P. C. Madhusudana, X. Yu, N. Birkbeck, Y. Wang, B. Adsumilli, and A. C. Bovik, “Subjective and objective quality assessment of high frame rate videos,” *IEEE Access*, vol. 9, pp. 108069–108082, 2021.
- [85] R. R. Rao, S. Göring, W. Robitza, B. Feiten, and A. Raake, “AVT-VQDB-UHD-1: A large scale video quality database for uhd-1,” in *2019 IEEE International Symposium on Multimedia (ISM)*. IEEE, 2019, pp. 17–177.
- [86] D. Y. Lee, S. Paul, C. G. Bampis, H. Ko, J. Kim, S. Y. Jeong, B. Homan, and A. C. Bovik, “A subjective and objective study of space-time subsampled video quality,” *IEEE Transactions on Image Processing*, vol. 31, pp. 934–948, 2021.
- [87] D. R. Bull and F. Zhang, *Intelligent image and video compression: communicating pictures*. Academic Press, 2021.
- [88] S. Winkler, “Analysis of public image and video databases for quality assessment,” *IEEE Journal of Selected Topics in Signal Processing*, vol. 6, no. 6, pp. 616–625, 2012.
- [89] F. M. Moss, K. Wang, F. Zhang, R. Baddeley, and D. R. Bull, “On the optimal presentation duration for subjective video quality assessment,” *IEEE Transactions on Circuits and Systems for Video Technology*, vol. 26, no. 11, pp. 1977–1987, 2015.
- [90] A. Mercat, M. Viitanen, and J. Vanne, “Uvg dataset: 50/120fps 4k sequences for video codec analysis and development,” in *Proceedings of the 11th ACM Multimedia Systems Conference*, 2020, pp. 297–302.

- [91] R. ITU-R BT, “500-14, methodologies for the subjective assessment of the quality of television images,” *International Telecommunication Union, Tech. Rep.*, 2019.
- [92] “Psychtoolbox-3,” <https://github.com/Psychtoolbox-3/Psychtoolbox-3>.
- [93] A. M. Van Dijk, J.-B. Martens, and A. B. Watson, “Quality assessment of coded images using numerical category scaling,” in *Advanced Image and Video Communications and Storage Technologies*, vol. 2451. SPIE, 1995, pp. 90–101.
- [94] T. Hoßfeld, C. Keimel, M. Hirth, B. Gardlo, J. Habigt, K. Diepold, and P. Tran-Gia, “Best practices for qoe crowdtesting: Qoe assessment with crowdsourcing,” *IEEE Transactions on Multimedia*, vol. 16, no. 2, pp. 541–558, 2013.
- [95] R. Péteri, S. Fazekas, and M. J. Huiskes, “DynTex: A comprehensive database of dynamic textures,” *Pattern Recognition Letters*, vol. 31, no. 12, pp. 1627–1632, 2010.
- [96] L. Zhang, L. Zhang, X. Mou, and D. Zhang, “FSIM: A feature similarity index for image quality assessment,” *IEEE transactions on Image Processing*, vol. 20, no. 8, pp. 2378–2386, 2011.
- [97] W. Xue, L. Zhang, X. Mou, and A. C. Bovik, “Gradient magnitude similarity deviation: A highly efficient perceptual image quality index,” *IEEE transactions on image processing*, vol. 23, no. 2, pp. 684–695, 2013.
- [98] E. Prashnani, H. Cai, Y. Mostofi, and P. Sen, “Pieapp: Perceptual image-error assessment through pairwise preference,” in *Proceedings of the IEEE Conference on Computer Vision and Pattern Recognition*, 2018, pp. 1808–1817.
- [99] S. Bosse, D. Maniry, K.-R. Müller, T. Wiegand, and W. Samek, “Deep neural networks for no-reference and full-reference image quality assessment,” *IEEE Transactions on image processing*, vol. 27, no. 1, pp. 206–219, 2017.
- [100] D. Danier, F. Zhang, and D. Bull, “FloLPIPS: A bespoke video quality metric for frame interpolation,” *arXiv preprint arXiv:2207.08119*, 2022.
- [101] A. Mittal, R. Soundararajan, and A. C. Bovik, “Making a “completely blind” image quality analyzer,” *IEEE Signal processing letters*, vol. 20, no. 3, pp. 209–212, 2012.
- [102] A. Mittal, M. A. Saad, and A. C. Bovik, “A completely blind video integrity oracle,” *IEEE Transactions on Image Processing*, vol. 25, no. 1, pp. 289–300, 2015.
- [103] M. A. Saad, A. C. Bovik, and C. Charrier, “Blind prediction of natural video quality,” *IEEE Transactions on Image Processing*, vol. 23, no. 3, pp. 1352–1365, 2014.
- [104] Z. Tu, Y. Wang, N. Birkbeck, B. Adsumilli, and A. C. Bovik, “UGC-VQA: Benchmarking blind video quality assessment for user generated content,” *IEEE Transactions on Image Processing*, vol. 30, pp. 4449–4464, 2021.
- [105] Z. Tu, X. Yu, Y. Wang, N. Birkbeck, B. Adsumilli, and A. C. Bovik, “RAPIQUE: Rapid and accurate video quality prediction of user generated content,” *IEEE Open Journal of Signal Processing*, vol. 2, pp. 425–440, 2021.
- [106] F. Zhang and D. R. Bull, “A perception-based hybrid model for video quality assessment,” *IEEE Transactions on Circuits and Systems for Video Technology*, vol. 26, no. 6, pp. 1017–1028, 2015.